Description and Validation of a Carbon Monoxide and Nitrous Oxide Instrument for High-Altitude Airborne Science (COMA)

Emma L. Yates[1,2], Levi M. Golston[1,3], James R. Podolske[1], Laura T. Iraci[1], Kristen E. Okorn[1,2,3],
Caroline Dang[1,2,3], Roy R. Johnson[1], James Eilers[1], Richard Kolyer[1], Ian Astley[4,*], J. Brian Leen[4,*]

[1] NASA Ames Research Center, Moffet Field, CA, USA
[2] Bay Area Environmental Research Institute, Moffett Field, CA, USA
[3] NASA Postdoctoral Program, NASA Ames Research Center, Moffett Field, CA, USA
[4] ABB Group, San Jose, CA, USA
[*] Now at Nikara Labs Inc., Mountain View, CA, USA

Correspondence to: Emma L. Yates (emma.l.yates@nasa.gov)

Abstract. In this work, we describe development of the Carbon monOxide Measurement from Ames (COMA) instrument for measurement of carbon monoxide (CO) and nitrous oxide (N_2O) aboard NASA's WB-57 high altitude research aircraft. While COMA has previously flown in the cabin of the NASA P-3 platform, here the instrument was modified to operate in a significantly different environment- an unpressurized pallet flying primarily above 12 km (40,000 ft). Modifications were made to the laser to allow for detection of CO and N_2O, ruggedization and thermal management were addressed, and a calibration system was designed to quantify the measurement stability in-flight. Testing was conducted in a thermal vacuum chamber to mimic anticipated ambient conditions experienced inside the WB-57 pallet bay and found electronic components remained within thermal limits. COMA successfully operated during nine unattended transit flights to and from South Korea and fifteen research flights during NASA's Asian summer monsoon Chemical & CLImate Project (ACCLIP) 2022 campaign, which was focused on studying the Asian summer monsoon anticyclone in the Western Pacific. The CO measurement has an overall uncertainty ranging between 4.1 ppb (at 50 ppb CO) and 5.6 ppb (at 200 ppb CO). N_2O has an overall uncertainty of 2.7 ppb (at 320 ppb N_2O). In addition, COMA observations were compared with two other in-situ CO instruments co-located on the WB-57: Carbon Monoxide Laser Detector (COLD) 2 and Airborne Carbonic Oxides and Sulfide Spectrometer (ACOS). Comparisons for 15 flights during the ACCLIP campaign indicate a range in slope of 1.10–1.15 for COLD2 vs. COMA and 0.94–1.10 for ACOS vs. COMA.

1 Introduction

The transport of trace gases and aerosols into and within the upper troposphere and lower stratosphere (UTLS) during the Asian summer monsoon was the focus of the Asian summer monsoon Chemical & CLImate Project (ACCLIP) field

campaign in summer 2022 (Honomichl & Pan, 2020; Pan et al., 2025). Carbon monoxide (CO) and nitrous oxide (N$_2$O) were key measurements during ACCLIP due to their long atmospheric lifetimes. CO is used as a tracer of boundary layer air transport and to infer airmass age (e.g. Pan et al., 2016; Park et al., 2009). Additionally, N$_2$O is a dominant ozone-
35 depleting substance (Ravishankara et al., 2009) with surface sources and stratospheric loss (Tian et al., 2020), which can indicate in-mixing of aged stratospheric air (e.g., Gonzalez et al., 2021; Hintsa et al., 1998). As such, understanding the transport mechanisms and behavior of CO and N$_2$O during the Asian summer monsoon is crucial for evaluating their impact on regional and global climate.

Given its importance, CO has been measured in numerous airborne field campaigns using different aircraft platforms and
40 several different measurement techniques. Established airborne measurements of CO and N$_2$O with fast instrument response time (seconds) frequently use high-precision infrared (IR) spectroscopic techniques to create spatially and temporally dense datasets. Existing spectroscopic sensor systems operating in the mid-IR use optical sources such as Quantum Cascade Lasers (QCLs) or Interband Cascade Lasers (ICLs) in conjunction with path length enhancement techniques such as multi-pass cells [Gvakharia, Vicicani, etc.] or Off-Axis Integrated Cavity Output Spectroscopy (OA-
45 ICOS) [Kloss] (Gvakharia et al., 2018; Kostinek et al., 2019; Pitt et al., 2016; Viciani et al., 2018). Systems operating in the near-IR and utilizing Cavity Ring-Down Spectroscopy (CRDS) have also been fielded (Filges et al., 2015). A detailed overview of these different methods can be found in Zellweger et al. (2012).

This paper describes the work undertaken to convert NASA's Carbon monOxide Measurement from Ames (COMA), a laboratory-based OA-ICOS instrument (Los Gatos Research (now ABB Ltd.)), into an airborne instrument capable of high-
50 altitude (18 km) airborne measurements of CO and N$_2$O. The airborne operational requirements were that COMA had to operate autonomously in an unpressurized, unheated payload bay of NASA's WB-57 aircraft while flying at altitudes up to 18 km for up to 5 hours of flight time during the ACCLIP campaign. Restrictions on the instrument design included: space/size, low operating pressure (~75 hPa), low in-flight temperature (-20 °C), high pre- and post-flight temperature (>30 °C) and humidity, and requirements for accurate and precise CO and N$_2$O measurements.

55 This work details the instrument testing, modifications, and final design of COMA, an instrument designed to meet operational requirements necessary for high altitude flights on NASA's WB-57. We also describe COMA's in-flight performance and operation and briefly discuss observations of CO and N$_2$O in the UTLS region during the Asian summer monsoon in summer 2022.

2 Instrument Design and Modifications

60 The operational requirements to fly in one half of a pallet for the payload bay of NASA's WB-57 included instrument size restrictions to physically fit within the space provided, inlet and operating pressure as low as 50 Torr (~75 hPa) when flying at 18 km, low in-flight temperature (-20 °C), but high pre- and post-flight temperature (>30 °C) and humidity during the ACCLIP field campaign. Operation in an unpressurized UTLS environment presents multiple challenges to instrument
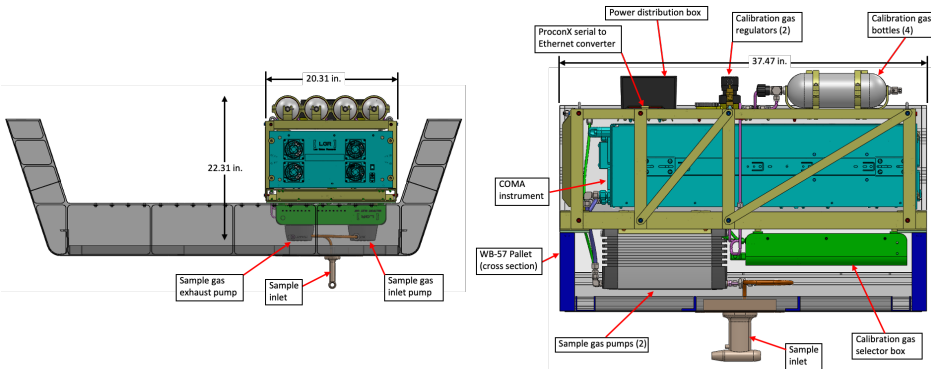
stability and performance, since the instrument is designed for ground-based operation. To address these challenges, the COMA instrument underwent significant modifications, followed by laboratory and environmental chamber testing to simulate instrument behavior under expected flight conditions.

2.1 Instrument Description

COMA is based on a laboratory-oriented OA-ICOS instrument (Los Gatos Research (now ABB Ltd.) GLA251-N2OCM) which detects a CO absorption feature as well as nearby N_2O and H_2O absorption features. The original instrument was manufactured for NASA Ames Research Center in December 2015. The un-modified instrument flew on NASA's P3 aircraft in a 19" rack within the pressurized cabin during the ObseRvations of Aerosols above CLouds and their intEractionS (ORACLES) field campaign in 2018, providing observations of CO and CO_2 on 41 flights up to 7 km altitude (Redemann et al., 2021).

In preparation for ACCLIP, some initial instrument modifications were made, including a computer stack upgrade and replacing the laser to one with increased sensitivity to CO. Changing the laser allowed for N_2O observations, but at the expense of removing the CO_2 channel. This was to accommodate the low values of CO expected to be observed in ACCLIP's UTLS-focused campaign. Other modifications included the installation of higher conductance vacuum control valves, increasing the measurement range of the sample gas temperature thermistor, and modification of the secondary laser temperature controller setpoint for the expected thermal environment. Sample cell pressure was adjusted to operate at 52.8 torr (70.4 hPa) to accommodate ambient UTLS pressures. Enclosure heaters and two 150 W box fans were added to the COMA payload to help reduce condensation on the optical windows and to stabilize the COMA enclosure temperature.

2.1.1 Payload Design

COMA was installed in a pallet for upload into NASA's WB-57 payload bay, as shown in Figure 1. COMA's external mounting structure (chassis) was Alodine treated aluminum and featured side rails to allow for easy installation. The total assembled payload (excluding the pallet) weighed 97.8 kg. The instrument was run from 115 VAC, 60 Hz power from the aircraft. A 28 VDC line for relay activation to power the instrument from the Experimental Control Panel (ECP) was added. The power distribution box contained breakers for the inlet heater, COMA analyzer, commercial multiport inlet unit (MIU), inlet pump, and a master switch. The external pump was controlled by COMA and was the default pump used (COMA switches from operating using an internal to external pump on initial startup). Addition of an 8-channel thermocouple temperature data logger (Madgetech TCTempX8LCD and Type K thermocouples) allowed for measurements of the thermal operating conditions experienced in-flight by COMA as shown in Figure 2.
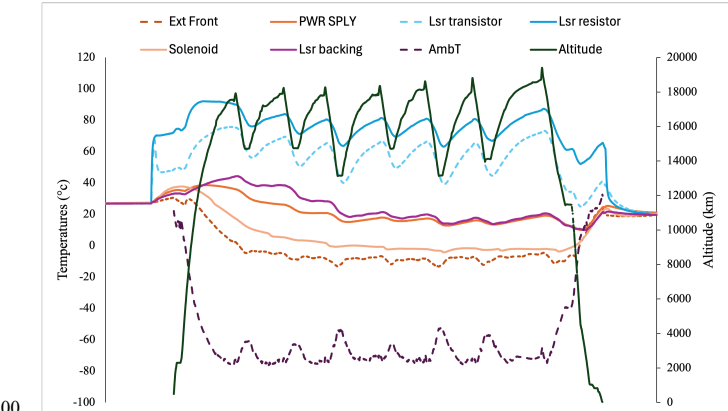
Figure 2: Typical operating thermal conditions experienced by COMA during ACCLIP research flights, data from 21 August 2022 (Research Flight # 11). The black line shows the aircraft altitude (right axis); other lines show measured temperatures at multiple locations inside and outside the COMA chassis. Orange-red (dash) = external front (Ext front), orange = power supply (PWR SPLY), light blue (dash) = laser transistor (Lsr transistor), blue = laser resistor (Lsr resistor), light orange – solenoid, purple = laser backing, purple (dash) = ambient temperature (Amb T).

2.1.2 Flow System

COMA used an inlet probe, which has previously flown on NASA's WB-57, from NASA Goddard Space Flight Center known as the "CAFE Inlet" (St. Clair et al., 2019) mounted on the underside of the pallet. The inlet includes a cartridge
110 heater (SunRod) controlled to 30 °C by a proportional controller (Minco CT335). Inside the payload bay, Teflon FEP or stainless-steel tubing carries the sample flow from the inlet to the instrument via an inlet diaphragm pump (KNF Group, NF N90 APE-W), relief valve (TAVCO 20 psia), and high-flow solenoid valve. The solenoid valve directs the sample air to one of the eight available ports on the MIU, which is programmed to control COMA's air sampling and calibration sampling pattern (discussed in Section 4.3). The inlet diaphragm pump, along with an internal (to COMA) pump and the
115 external (to COMA) exhaust pump (KNF Group, NF N90 APE-W) pull the sample through COMA and exhaust it to the ambient atmosphere. COMA contains internal valves that maintain a pressure of 52.8 Torr within COMA's sampling cell. A diagram of COMA's flow system is shown in Figure 3.
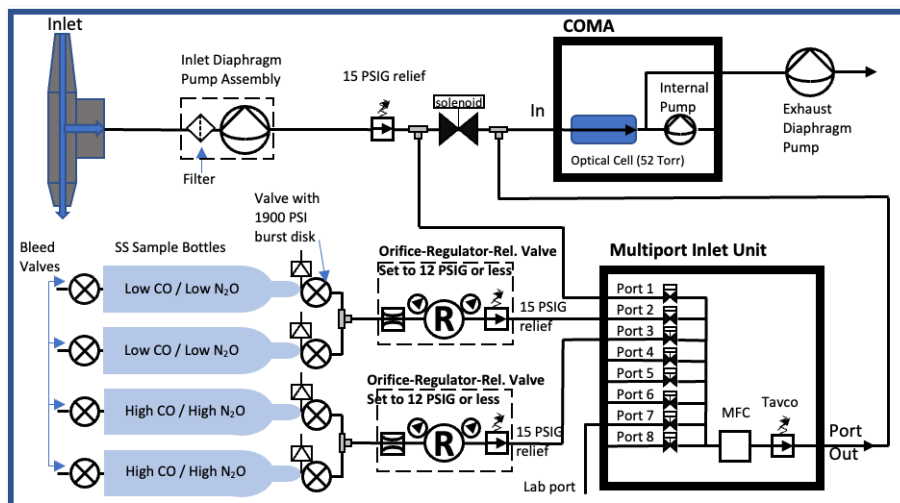

Figure 3: COMA flow diagram.

120
COMA's in-flight calibration system consisted of four Swagelok double-ended stainless steel cylinders (304L-HDF4-1000) with 1800 PSI maximum allowable working pressure (MAWP) and 1000 PSIG maximum operating pressure (MOP). Prior to the ACCLIP campaign deployment, the in-flight cylinders were filled from one of four source cylinders: two primary NOAA Global Monitoring Laboratory whole air standards, certified by the WMO Central Calibration Laboratory for CO
125 (Novelli et a., 1991) and N_2O (Hall et al., 2007) (low CO standard "NOAA 1", (tank # CC745344, CO ~51.77 ppb ±0.94,

N_2O ~265.89 ppb ±0.03 and high CO standard "NOAA 2", (tank # CC746190, CO ~164.34 ppb ±1.84, N_2O~348.06 ppb ±0.05), and two secondary standards ("Matheson 1", ~200 ppb each of CO and N_2O, and "Matheson 2", ~1000 ppb each of CO and N_2O). The NOAA standards are referenced on the WMO CO_X2014A scale for CO and the NOAA-2006A scale for N_2O. Further details on the calibration scales can be found at https://gml.noaa.gov/ccl/refgas.html. Only two

130 standard cylinders were open at any one time (the other two had valve locks installed on the unopened cylinders to prevent leakage). The two NOAA-filled cylinders were the first to be sampled by COMA during in-flight calibrations before beginning to sample the secondary standards. The standards were deployed during the field campaign, which allowed the in-flight calibration system to be re-filled with the secondary standards and sampled throughout the duration of the ACCLIP deployment.

135 **2.1.3 Telemetry**

COMA was required to run autonomously onboard the WB-57. The instrument could be controlled (on/off) by the Science Equipment Operator located in the rear cockpit to power cycle the instrument. Bandwidth to communicate with the instrument in-flight was limited. To address this, we developed a communication and processing software for real-time monitoring on the ground, consisting of a Python script which ran on the analyzer to access data files and output 1 Hz user

140 data protocol (UDP) packets. It also included a proconX SERIP-100 serial-to-ethernet converter as backup system, which sent UDP packets for real time monitoring on the ground. In addition, NASA's Mission Tools Suite (MTS) was used to communicate to the ground while in-flight (https://airbornescience.nasa.gov/tracker/).

2.2 Instrument Performance

2.2.1 Environmental Chamber Testing

145 Prior to deployment, COMA was extensively tested in the NASA Ames Research Center Engineering Evaluation Laboratory (EEL). The environmental chamber testing plans centered around two main concerns. First, the thermal stability of the instrument's components were tested to ensure safe operation of the laser and other components under UTLS-like conditions. Second, the stability of the instrument was tested by sampling from a standard gas mixture while simulating UTLS conditions.

150 In the environmental chamber, seven thermocouples were placed inside the COMA instrument, one along the middle dividing panel inside sensor (Figure 4: mid-rib), and at six locations considered critical or at risk of overheating. Figure 4 shows the thermal performance of COMA's individual components during a simulated UTLS flight, when the chamber altitude (pressure) was varied (Figure 4: black line, secondary y-axis). Results from the thermal testing showed that at altitudes up to 18 km, components did not become unstable or overheat outside of the expected operational ranges identified
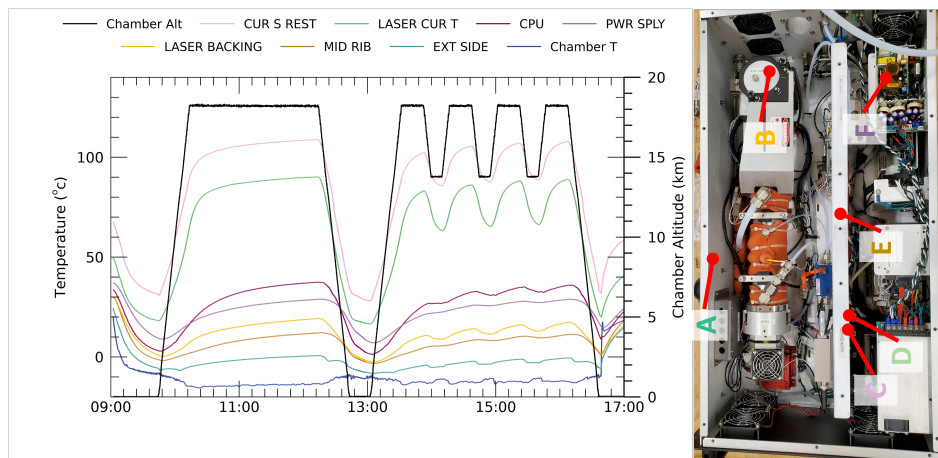
155 for these components.

6

Figure 4: Environmental chamber timeseries showing COMA's component temperatures during a simulated UTLS flight conducted on 20 May 2022 (right). Corresponding thermocouple locations are shown on the right, external side = EXT SIDE (A), laser backing (B), laser current sensing resistor = CUR S REST (C), laser current temperature = LASER CUR T (D), internal dividing panel = MID-RIB (E), and power supply = PWR SPLY (F).

Allan deviation (Allan, 1987) was used as a metric of COMA's stability as shown in Figure 5, which presents the Allan deviation as a function of averaging time to illustrate how precision changes based on data averaging. The results show a laboratory 1 Hz precision of ~0.13 ppb for CO and ~0.19 ppb for N_2O. Precision improves with increased data averaging during standard sampling in the laboratory (blue) up to ~1000 s, after which additional time averaging has little benefit. In the environmental chamber, under conditions shown in Figure 4, precision is similar at 1 Hz and improves with increased averaging at approximately the same rate of change as in the laboratory up to 10 s, after which the improvements in precision are at a slower rate of change, likely due to noise or additional uncertainty in the measurements due to changing operational (chamber temperature and pressure) conditions.
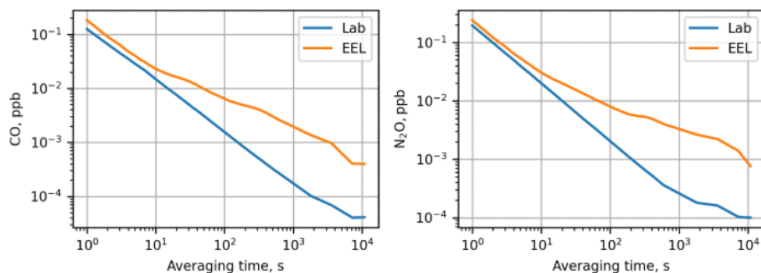
7

Figure 5. Allan deviation results, comparing data collected in lab (blue) and an environmental chamber (EEL, orange) during standard sampling for CO (left) and N_2O (right). Under both conditions, 1 Hz precision ~ 0.1 – 0.2 ppb for both gases. See Figure 4 for chamber pressure and temperature details.

180 **2.2.2 Instrument Linearity**

Linearity assessments were performed using a flow mixing system equipped with high accuracy mass flow controllers (Alicat Scientific Inc., MC-1SLP-D, (most recent calibration, reported accuracy was ±0.6 % of reading (3 Nov 2021)) and OMEGA Engineering inc., FMA-2602A, (most recent calibration, reported accuracy was ±0.4 % of reading (11 Jul 2021)). A secondary synthetic CO standard (~1000 ppb each of CO and N_2O) and a zero-air standard were used to perform the

185 linearity mixing analysis. The linearity assessment for COMA is shown in Figure 6 and demonstrates that COMA is highly linear over a wide range of CO and N_2O mixing ratios. Figure 6 shows COMA to be linear (slope of 1.00) to within 0.1% between 25-1000 ppb CO and linear (slope of 1.00) within 0.1% between 25-850 ppb N_2O, with the largest uncertainty equal to the reported accuracies of the flow meters stated above.
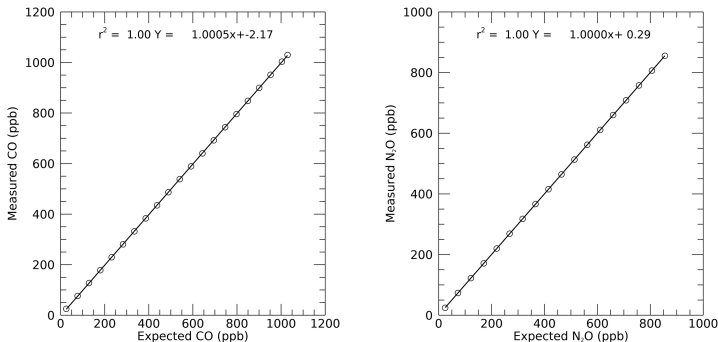
Deleted: .

Figure 6: COMA Instrument linearity for CO (left) and N₂O (right) as performed under laboratory conditions on 20 October 2023.

2.2.3 Instrument Calibration and Measurement Uncertainty

Calibration to NOAA standards was applied (see Section 2.1.2) using data collected at ground level throughout the campaign as well as after to help account for time drift in the instrument. Outliers, which deviated from the mean by more than 4 standard deviations were removed. Multivariate linear regressions with time and measured concentration as dependent variables were applied for both CO and N₂O. Slight degradation in instrument response was observed over the course of the campaign and was accounted for with the inclusion of an elapsed time term in the final calibrations. The estimation of overall accuracy of CO includes small contributions due to accuracy of the standard gases but was dominated by the residuals remaining after this calibration to NOAA standards. Overall accuracy for CO was determined to be ± 3.8 ppb over the calibration range. Accuracy for N₂O is comprised equally of the contributions from the residuals after calibration to NOAA standards (1.0 ppb) and NOAA scale uncertainty (0.31 %). Given the relatively small range of N₂O values observed in the field, overall accuracy in N₂O can be approximated by the value of +/- 1.4 ppb, as calculated at N₂O = 320 ppb.

The in-flight calibration system ran a cycle of 60 s of low-mixing ratio calibration gas, followed by 60 s of high mixing ratio gas periodically throughout each flight. Figure 7 shows the results from in-flight calibrations for CO (bottom) and N₂O (top) during the ACCLIP deployment for primary whole air NOAA standards (left) and secondary synthetic standards (right). Note that only the NOAA standards were used for linear calibration fits; the secondary synthetic standards were only used for internal assessment. The intra- and inter-flight variability among flight calibrations give an indication of the in-flight instrument 1σ precision. The standard deviations of observations at three different mixing ratios were seen to vary slightly with mixing ratio as shown in Equation 1 and Equation 2. For example, At 320 ppb N₂O precision = 2.3 ppb (equivalent to 0.7 %). At 50 ppb CO precision = 1.4 ppb (equivalent to 2.8 %), while at 200 ppb CO precision = 4.1 ppb (equivalent to 2.1 %). Readers should use discretion if extrapolation of precision is required outside the range used to determine these equations (CO: 48-203 ppb; N2O: 195 – 345 ppb).

$$CO\ precision\ =\ 1.79x10^{-02} \times CO\ (ppb)\ +\ 0.50 \qquad \text{Equation 1}$$

$$N_2O\ precision\ =\ 8.05x10^{-03} \times N_2O\ (ppb) - 0.25 \qquad \text{Equation 2}$$

Overall uncertainty is determined by the square root of the sum of the squares of the accuracy and precision terms. If desired, total uncertainty for each measurement can be calculated from individual terms. Under flight conditions at 320 ppb N₂O total uncertainty is 2.7 ppb. At 50 ppb CO total uncertainty is 4.1 ppb; at 200 ppb CO total uncertainty is 5.6 ppb.
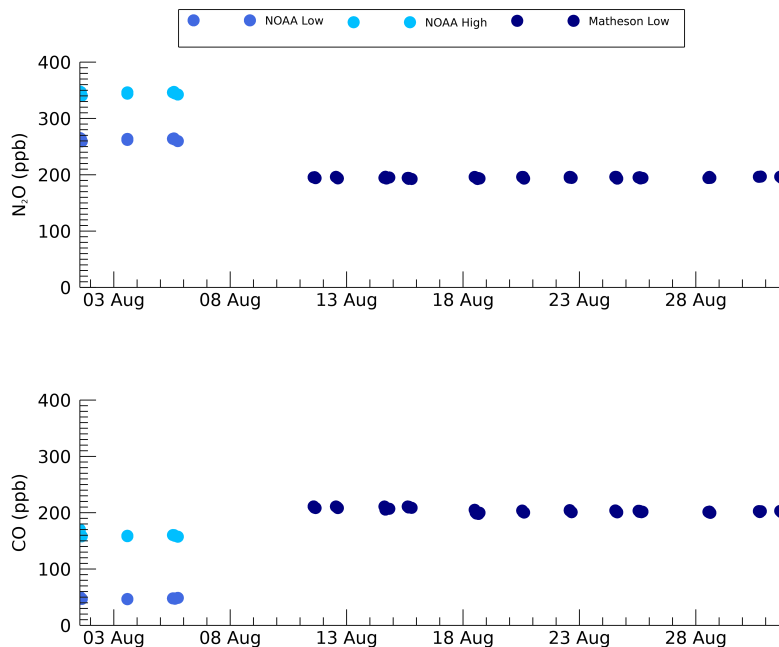
Moved (insertion) [1]

Figure 7: Mean value from individual in-flight calibration periods for CO (bottom) and N₂O (top) during the ACCLIP deployment for primary whole air NOAA standards (prior to August 8, 2022) and secondary Matheson synthetic standards (after August 11, 2022). The standard deviation of each calibration mean value is significantly smaller than the size of the symbol plotted. Note, the primary whole air standards (NOAA) were sampled during in-flight calibrations prior to August 8, 2022. Once these were exhausted, the secondary standards (Matheson) were used for in-flight calibrations on/after August 11, 2022.

2.2.4   Data Processing

In addition to applying the calibration equations described in Section 2.2.3, several steps were taken to ensure the quality of the reported atmospheric observations of CO and N₂O. Measurements recorded during periodic calibration cycles and up to a minute of data before and after were removed, as were measurements before and during take-off and after landing. A time lag is present in the raw data due to combination of physical effects and clock offsets, which were accounted for by determining a median offset for each flight by correlation to an additional CO instrument (COLD2) onboard the WB-57. When COMA's measurement cell pressure deviated from the median pressure by more than 0.25%, N₂O data were omitted, and CO data were omitted on a case-by-case basis. (CO measurements were more robust against cell pressure oscillations, but not immune.) Additional deviations from nominal operating conditions were evaluated on a case-by-case basis.

Moved up [1]: Overall uncertainty is determined by the square root of the sum of the squares of the accuracy and precision terms. If desired, total uncertainty for each measurement can be calculated from individual terms. Under flight conditions at 320 ppb N₂O total uncertainty is 2.7 ppb. At 50 ppb CO total uncertainty is 4.1 ppb; at 200 ppb CO total uncertainty is 5.6 ppb.

3 COMA In-flight Data

COMA flew onboard NASA's WB-57 on four test flights (TF) from Ellington Field, TX in summer 2021, one functional check flight and two test flights in Ellington Field, TX in July 2022, five outbound transit flights from Ellington Field, TX,
245 USA to Osan Air Base, South Korea, 15 research flights (RF) from Osan Air Base and four return transit flights to Ellington Field, TX, USA. Data is archived and publicly available at the NASA Langley Research Center (LaRC) Distributed Active Archive Center (DAAC) (https://www-air.larc.nasa.gov/cgi-bin/ArcView/acclip.2022).

The WB-57 typically profiled multiple times through the UTLS during each research flight, resulting in vertical profiles of CO and N_2O. Figure 7 shows a summary of observations of N_2O and CO reported by COMA plotted by altitude and colored
250 by flight date for ACCLIP campaign research flights from Osan, South Korea. General observations include day-to-day variability in CO and N_2O within the boundary layer (<~2 km). Within the free-troposphere (~2.5 to 12.5 km) N_2O is well-mixed, with little day-to-day variability, however there is more variability observed in CO. The UTLS region (~12.5 to 16 km), shows highly variable CO, with the interception of lofted pollution originating from convective influences over Asia during different flights. In contrast, N_2O remains well-mixed in this altitude region. Decreasing profiles of both CO and
255 N_2O were observed within the stratosphere (>~16 km).
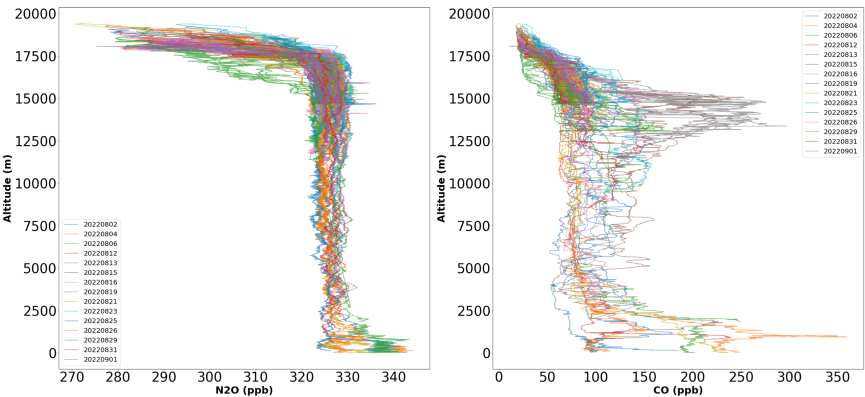

Figure 8: Vertical profiles of all N_2O (left) and CO (right) measurements taken by COMA during the ACCLIP campaign research flights from Osan, Korea in July and August 2022.

3.1 Data Comparison with COLD2 and ACOS

260 During the ACCLIP campaign, two other instruments were onboard NASA's WB-57 that measured CO: Carbon Monoxide Laser Detector (COLD) 2 and Airborne Carbonic Oxides and Sulfide Spectrometer (ACOS). COLD2, operated by CNR-INO (CNR National Institute of Optics), is a mid-infrared quantum cascade laser spectrometer that has previously flown on an M55 aircraft during StratoClim (Stratospheric and upper tropospheric processes for better climate predictions)

(Viciani et al., 2018). ACOS is a NOAA-operated, Off-Axis Integrated Cavity Output Spectrometer (ICOS) that measures
carbonyl sulfide (OCS) and CO (Gurganus et al., 2024).

Figure 9 shows the CO data comparison as a linear regression and demonstrates an excellent overall agreement between the three CO instruments. The cross plot shows the correlation of the 1 Hz CO measurements with ACOS and COLD2 CO plotted on the vertical axis and COMA CO on the horizontal axis, with a slope of 1.06 for COLD2 ($r^2 = 0.99$) and 1.01 for ACOS ($r^2 = 0.98$), indicating strong agreement throughout the ACCLIP field campaign. Comparisons of the 15 individual flights from the campaign indicate a range in slope of 1.02-1.08 for COLD2 and 0.89–1.10 for ACOS.
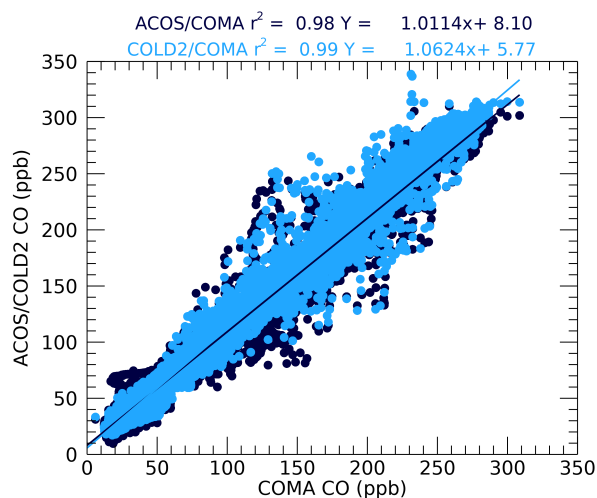

Figure 9: Linear regression of ACOS and COLD2 vs COMA for all 15 ACCLIP science flights.

4 Conclusion

The NASA COMA instrument provides high-sensitivity measurements of CO and N_2O from ground-level to an altitude of ~18 km. COMA flew onboard NASA's WB-57 during 24 flights, supporting the ACCLIP field campaign based in Korea during 2022. COMA data from this campaign is archived and publicly available (https://www-air.larc.nasa.gov/cgi-bin/ArcView/acclip.2022).

During ACCLIP, COMA flew primarily between 12 and 19 km within an unpressurized pallet of the WB-57. To operate successfully in these conditions, significant modifications were made to the original laboratory-oriented instrument,

followed by laboratory and environmental chamber testing to simulate instrument behavior under expected flight conditions.

This paper details the COMA design modifications, including the installation into the WB-57 payload pallet required for flight. Details of internal instrument modifications and changes to operational parameters are detailed in Section 2. External modifications to COMA to accommodate flights in the UTLS region included additional heaters and fans to help reduce condensation and for thermal management. An in-flight calibration system was added to the COMA payload to allow an evaluation of COMA in-flight performance, and an MIU to allow gas sampling selection (e.g. inlet, calibration standard, detailed in Section 2.1.2).

COMA instrument performance was assessed through extensive laboratory and environmental chamber testing (detailed in Section 2.2). This testing included assessments of COMA operation under simulated UTLS conditions, linearity assessment, assessment of laboratory and in-flight COMA calibrations, and data comparison of COMA to two independent instruments measuring CO (COLD2 and ACOS). Overall, the instrument achieved an uncertainty during ACCLIP of 2.7 ppb N_2O (at 320 ppb) and 5.6 ppb CO (at 200 ppb). COMA's successful integration aboard NASA's WB-57, demonstrated field performance, and favorable comparison to other independent instruments enable a new CO and N_2O capability for airborne science measurements in the upper troposphere and lower stratosphere.

Author contributions: JRP and LTI supervised the project. JE, RRJ, and JRP led design and integration onto the WB-57 aircraft. JBL, IA, JRP, and RRJ contributed towards environmental chamber testing and system design. LMG, JRP, RRJ, RK, LTI, KEO, CD, and ELY were involved in lab and field investigation. KEO, JRP, and LMG curated the COMA data, KEO and LMG wrote software used. LMG and ELY wrote the original draft, which was revised with feedback from all authors.

Competing interests: The authors declare that they have no conflict of interest.

References

Allan, D. W.: Should the Classical Variance be Used as a Basic Measure in Standards Metrology?, IEEE Transactions on Instrumentation and Measurement, vol. IM-36, no. 2, pp. 646–654, June 1987, doi: 10.1109/TIM.1987.6312761, 1987.

Baer, D. S., Paul, J. B., Gupta, M., and O'Keefe, A.: Sensitive absorption measurements in the near-infrared region using off-axis integrated-cavity-output spectroscopy, Appl. Phys. B Lasers Opt., 75, 261–265, https://doi.org/10.1007/s00340-002-0971-z, 2002.

Barret, B., Sauvage, B., Bennouna, Y., and Le Flochmoen, E.: Upper-tropospheric CO and O3 budget during the Asian summer monsoon, Atmospheric Chem. Phys., 16, 9129–9147, https://doi.org/10.5194/acp-16-9129-2016, 2016.

Barrett, P. A., Abel, S. J., Coe, H., Crawford, I., Dobracki, A., Haywood, J., Howell, S., Jones, A., Langridge, J., McFarquhar, G. M., Nott, G. J., Price, H., Redemann, J., Shinozuka, Y., Szpek, K., Taylor, J. W., Wood, R., Wu, H., Zuidema, P., Bauguitte, S., Bennett, R., Bower, K., Chen, H., Cochrane, S., Cotterell, M., Davies, N., Delene, D., Flynn, C., Freedman, A., Freitag, S., Gupta, S., Noone, D., Onasch, T. B., Podolske, J., Poellot, M. R., Schmidt, S., Springston, S., Sedlacek III, A. J., Trembath, J., Vance, A., Zawadowicz, M. A., and Zhang, J.: Intercomparison of airborne and surface-based measurements during the CLARIFY, ORACLES and LASIC field experiments, Atmospheric Meas. Tech., 15, 6329–6371, https://doi.org/10.5194/amt-15-6329-2022, 2022.

Bernath, P. F., Yousefi, M., Buzan, E., and Boone, C. D.: A Near-Global Atmospheric Distribution of N_2O Isotopologues: N_2O Isotopologues, Geophys. Res. Lett., 44, 10,735–10,743, https://doi.org/10.1002/2017GL075122, 2017.

Bourgeois, I., Peischl, J., Neuman, J. A., Brown, S. S., Allen, H. M., Campuzano-Jost, P., Coggon, M. M., DiGangi, J. P., Diskin, G. S., Gilman, J. B., Gkatzelis, G. I., Guo, H., Halliday, H. A., Hanisco, T. F., Holmes, C. D., Huey, L. G., Jimenez, J. L., Lamplugh, A. D., Lee, Y. R., Lindaas, J., Moore, R. H., Nault, B. A., Nowak, J. B., Pagonis, D., Rickly, P. S., Robinson, M. A., Rollins, A. W., Selimovic, V., St. Clair, J. M., Tanner, D., Vasquez, K. T., Veres, P. R., Warneke, C., Wennberg, P. O., Washenfelder, R. A., Wiggins, E. B., Womack, C. C., Xu, L., Zarzana, K. J., and Ryerson, T. B.: Comparison of airborne measurements of NO, NO_2, HONO, NO_y, and CO during FIREX-AQ, Atmospheric Meas. Tech., 15, 4901–4930, https://doi.org/10.5194/amt-15-4901-2022, 2022.

Diskin, G. S., Podolske, J. R., Sachse, G. W., and Slate, T. A.: Open-path airborne tunable diode laser hygrometer, International Symposium on Optical Science and Technology, Seattle, WA, 4817, 196–204, https://doi.org/10.1117/12.453736, 2002.

Filges, A., Gerbig, C., Chen, H., Franke, H., Klaus, C., and Jordan, A.: The IAGOS-core greenhouse gas package: a measurement system for continuous airborne observations of CO_2, CH_4, H_2O and CO, Tellus B Chem. Phys. Meteorol., 67, 27989–**28008**, https://doi.org/10.3402/tellusb.v67.27989, 2015.

Gomez-Pelaez, A. J., Ramos, R., Cuevas, E., Gomez-Trueba, V., and Reyes, E.: Atmospheric CO2, CH4, and CO with the CRDS technique at the Izaña Global GAW station: instrumental tests, developments, and first measurement results, Atmospheric Meas. Tech., 12, 2043–2066, https://doi.org/10.5194/amt-12-2043-2019, 2019.

Gonzalez, Y., Commane, R., Manninen, E., Daube, B. C., Schiferl, L. D., McManus, J. B., McKain, K., Hintsa, E. J., Elkins, J. W., Montzka, S. A., Sweeney, C., Moore, F., Jimenez, J. L., Campuzano Jost, P., Ryerson, T. B., Bourgeois, I., Peischl, J., Thompson, C. R., Ray, E., Wennberg, P. O., Crounse, J., Kim, M., Allen, H. M., Newman, P. A., Stephens, B. B., Apel, E. C., Hornbrook, R. S., Nault, B. A., Morgan, E., and Wofsy, S. C.: Impact of stratospheric air and surface emissions on tropospheric nitrous oxide during ATom, Atmos. Chem. Phys., 21, 11113–11132, https://doi.org/10.5194/acp-21-11113-2021, 2021.

Gottschaldt, K.-D., Schlager, H., Baumann, R., Bozem, H., Eyring, V., Hoor, P., Jöckel, P., Jurkat, T., Voigt, C., Zahn, A., and Ziereis, H.: Trace gas composition in the Asian summer monsoon anticyclone: a case study based on aircraft observations and model simulations, Atmospheric Chem. Phys., 17, 6091–6111, https://doi.org/10.5194/acp-17-6091-2017, 2017.

Gurganus, C., Rollins, A. W., Waxman, E., Pan, L. L., Smith, W. P., Ueyama, R., Feng, W., Chipperfield, M. P., Atlas, E. L., Schwarz, J. P., Lee, S., Thornberry, T. D.: Highlighting the impact of anthropogenic OCS emissions on the stratospheric budget with in-situ observations, ESS Open Archive, doi: 10.22541/essoar.172801406.62154439/v1, 2024.

Gvakharia, A., Kort, E. A., Smith, M. L., and Conley, S.: Testing and evaluation of a new airborne system for continuous N_2O, CO_2, CO, and H_2O measurements: the Frequent Calibration High-performance Airborne Observation System (FCHAOS), Atmospheric Meas. Tech., 11, 6059–6074, doi: 10.5194/amt-11-6059-2018, 2018.

Hall, B. D., Dutton, G. S., and Elkins, J. W.: The NOAA nitrous oxide standard scale for atmospheric observations, J. Geophys. Res., 112, D9, https://doi.org/10.1029/2006JD007954, 2007.

Hintsa, E., Boering, K. A.,Weinstock, E. M., Anderson, J. G., Gary, B. L., Pfister, L., Daube, B. C., Wofsy, S. C., Loewenstein, M., Podolske, J. R., Margitan, J. J., and Bu, T. T.: Troposphere-to stratosphere transport in the lowermost stratosphere from measurements of H_2O, CO, N_2O and O_3, Geosphys. Res. Lett., 25, 14, 2655–2658, https://doi.org/10.1029/98GL01797, 1998.

Honomichl, S. B., and Pan, L. L.: Transport from the Asian Summer Monsoon Anticyclone Over the Western Pacific, J. Geophys. Res., 125, e2019JD032094, https://doi.org/10.1029/2019JD032094, 2020.

Kostinek, J., Roiger, A., Davis, K. J., Sweeney, C., DiGangi, J. P., Choi, Y., Baier, B., Hase, F., Groß, J., Eckl, M., Klausner, T., Butz, A.: Adaptation and performance assessment of a quantum and interband cascade laser spectrometer for

simultaneous airborne in situ observation of CH_4, C_2H_6, CO_2, CO and N_2O, Atmospheric Measurement Techniques,

375   12, 1767-1783, doi: 10.5194/amt-12-1767-2019, 2019.

Kloss, C., Tan, V., Leen, J. B., Madsen, G. L., Gardner, A., Du, X., Kulessa, T., Schillings, J., Schneider, H., Schrade, S., Qiu, C., and von Hobe, M.: Airborne Mid-Infrared Cavity enhanced Absorption spectrometer (AMICA), Atmospheric Meas. Tech., 14, 5271–5297, https://doi.org/10.5194/amt-14-5271-2021, 2021.

Nédélec, P., Cammas, J.-P., Thouret, V., Athier, G., Cousin, J.-M., Legrand, C., Abonnel, C., Lecoeur, F., Cayez, G., and

380   Marizy, C.: An improved infrared carbon monoxide analyser for routine measurements aboard commercial Airbus aircraft: technical validation and first scientific results of the MOZAIC III programme, Atmospheric Chem. Phys., 3, 1551–1564, https://doi.org/10.5194/acp-3-1551-2003, 2003.

Nédélec, P., Blot, R., Boulanger, D., Athier, G., Cousin, J.-M., Gautron, B., Petzold, A., Volz-Thomas, A., and Thouret, V.: Instrumentation on commercial aircraft for monitoring the atmospheric composition on a global scale: the IAGOS

385   system, technical overview of ozone and carbon monoxide measurements, Tellus B Chem. Phys. Meteorol., 67, 27791–27808, https://doi.org/10.3402/tellusb.v67.27791, 2015.

Novelli, P. C.: CO in the atmosphere: measurement techniques and related issues, Chemosphere - Glob. Change Sci., 1, 115–126, https://doi.org/10.1016/S1465-9972(99)00013-6, 1999.

Novelli, P. C., Elkins, E. W., Steele, L. P.: The development and evaluation of a gravimetric reference scale for

390   measurements of atmospheric carbon monoxide, J. Geophys, Res., 96, D7, https://doi.org/10.1029/91JD01108, 1991.

Pan, L. L., Honomichl, S. B., Kinnison, D. E., Abalos, M., Randel, W. J., Bergman, J. W., and Bian, J.: Transport of chemical tracers from the boundary layer to stratosphere associated with the dynamics of the Asian summer monsoon, J. Geophys. Res. Atmospheres, 121, 14, 159-174, https://doi.org/10.1002/2016JD025616, 2016.

Pan, L. L.: The Asian Summer Monsoon Chemical and Climate Impacts Project (ACCLIP): An Overview, in preparation

395   (submission intended in March 2025).

Park, M., Randel, W. J., Emmons, L. K., Bernath, P. F., Walker, K. A., and Boone, C. D.: Chemical isolation in the Asian monsoon anticyclone observed in Atmospheric Chemistry Experiment (ACE-FTS) data, Atmospheric Chem. Phys., 8, 757–764, https://doi.org/10.5194/acp-8-757-2008, 2008.

Park, M., Randel, W. J., Emmons, L. K., and Livesey, N. J.: Transport pathways of carbon monoxide in the Asian summer

400   monsoon diagnosed from Model of Ozone and Related Tracers (MOZART), J. Geophys. Res. 114, D08303, https://doi.org/10.1029/2008JD010621, 2009

Paul, J. B., Lapson, L., and Anderson, J. G.: Ultrasensitive absorption spectroscopy with a high-finesse optical cavity and off-axis alignment, Appl. Opt., 40, 4904–4910, https://doi.org/10.1364/AO.40.004904, 2001.

Pitt, J. R., Le Breton, M., Allen, G., Percival, C. J., Gallagher, M. W., Bauguitte, S. J.-B., O'Shea, S. J., Muller, J. B. A.,

405   Zahniser, M. S., Pyle, J., and Palmer, P. I.: The development and evaluation of airborne in situ N_2O and CH_4 sampling using a quantum cascade laser absorption spectrometer (QCLAS), Atmospheric Meas. Tech., 9, 63–77, https://doi.org/10.5194/amt-9-63-2016, 2016.

Provencal, R., Gupta, M., Owano, T. G., Baer, D. S., Ricci, K. N., O'Keefe, A., and Podolske, J. R.: Cavity-enhanced quantum-cascade laser-based instrument for carbon monoxide measurements, Appl. Opt., 44, 6712–6717, https://doi.org/10.1364/AO.44.006712, 2005.

Ravishkara, A. R., Daniel, J. S., Portmann R. W.: Nitrous Oxide (N_2O): The Dominant Ozone-Depleting Substance Emitted in the 21st Century, Science, 326, 5929, 123-125, doi: 10.1126/science.1176985, 2009.

Redemann, J., Wood, R., Zuidema, P., Doherty, S. J., Luna, B., LeBlanc, S. E., Diamond, M. S., Shinozuka, Y., Chang, I. Y., Ueyama, R., Pfister, L., Ryoo, J.-M., Dobracki, A. N., da Silva, A. M., Longo, K. M., Kacenelenbogen, M. S., Flynn, C. J., Pistone, K., Knox, N. M., Piketh, S. J., Haywood, J. M., Formenti, P., Mallet, M., Stier, P., Ackerman, A. S., Bauer, S. E., Fridlind, A. M., Carmichael, G. R., Saide, P. E., Ferrada, G. A., Howell, S. G., Freitag, S., Cairns, B., Holben, B. N., Knobelspiesse, K. D., Tanelli, S., L'Ecuyer, T. S., Dzambo, A. M., Sy, O. O., McFarquhar, G. M., Poellot, M. R., Gupta, S., O'Brien, J. R., Nenes, A., Kacarab, M., Wong, J. P. S., Small-Griswold, J. D., Thornhill, K. L., Noone, D., Podolske, J. R., Schmidt, K. S., Pilewskie, P., Chen, H., Cochrane, S. P., Sedlacek, A. J., Lang, T. J., Stith, E., Segal-Rozenhaimer, M., Ferrare, R. A., Burton, S. P., Hostetler, C. A., Diner, D. J., Seidel, F. C., Platnick, S. E., Myers, J. S., Meyer, K. G., Spangenberg, D. A., Maring, H., and Gao, L.: An overview of the ORACLES (ObseRvations of Aerosols above CLouds and their intEractionS) project: aerosol–cloud–radiation interactions in the southeast Atlantic basin, Atmos. Chem. Phys., 21, 1507–1563, https://doi.org/10.5194/acp-21-1507-2021, 2021.

Scharffe, D., Slemr, F., Brenninkmeijer, C. A. M., and Zahn, A.: Carbon monoxide measurements onboard the CARIBIC passenger aircraft using UV resonance fluorescence, Atmospheric Meas. Tech., 5, 1753–1760, https://doi.org/10.5194/amt-5-1753-2012, 2012.

Schiller, C. L., Bozem, H., Gurk, C., Parchatka, U., Königstedt, R., Harris, G. W., Lelieveld, J., and Fischer, H.: Applications of quantum cascade lasers for sensitive trace gas measurements of CO, CH_4, N_2O and HCHO, Appl. Phys. B, 92, 419–430, https://doi.org/10.1007/s00340-008-3125-0, 2008.

St. Clair, J. M., Swanson, A. K., Bailey, S. A., and Hanisco, T. F.: CAFE: a new, improved nonresonant laser-induced fluorescence instrument for airborne in situ measurement of formaldehyde, Atmospheric Meas. Tech., 12, 4581–4590, https://doi.org/10.5194/amt-12-4581-2019, 2019.

Tian, H., Xu, R., Canadell, J.G. *et al.* A comprehensive quantification of global nitrous oxide sources and sinks. *Nature* 586, 248–256 (2020). https://doi.org/10.1038/s41586-020-2780-0

Viciani, S., Montori, A., Chiarugi, A., and D'Amato, F.: A Portable Quantum Cascade Laser Spectrometer for Atmospheric Measurements of Carbon Monoxide, Sensors, 18, 2380–2398, https://doi.org/10.3390/s18072380, 2018.

Zellweger, C., Steinbrecher, R., Laurent, O., Lee, H., Kim, S., Emmenegger, L., Steinbacher, M., and Buchmann, B.: Recent advances in measurement techniques for atmospheric carbon monoxide and nitrous oxide observations, Atmospheric Meas. Tech., 12, 5863–5878, https://doi.org/10.5194/amt-12-5863-2019, 2019.